

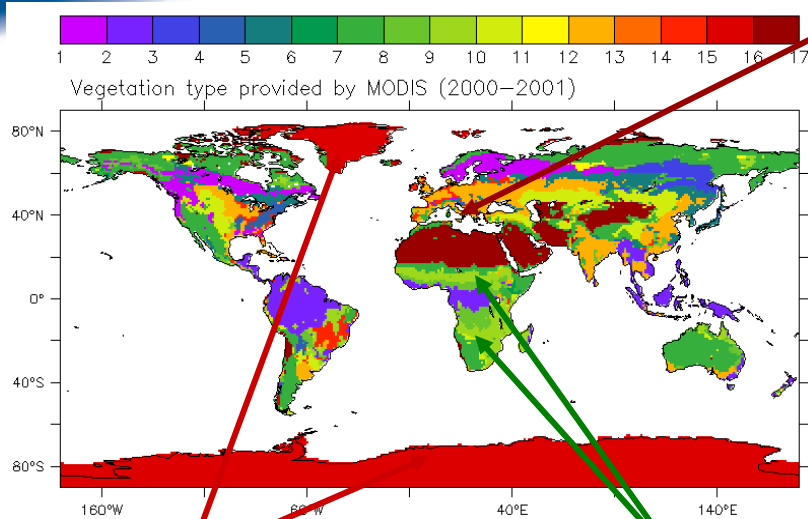
# Infrared continental surface emissivity spectra retrieved from IASI observations

*E. Péquignot<sup>a</sup>, A. Chédin<sup>b</sup>, N. A. Scott<sup>b</sup>*

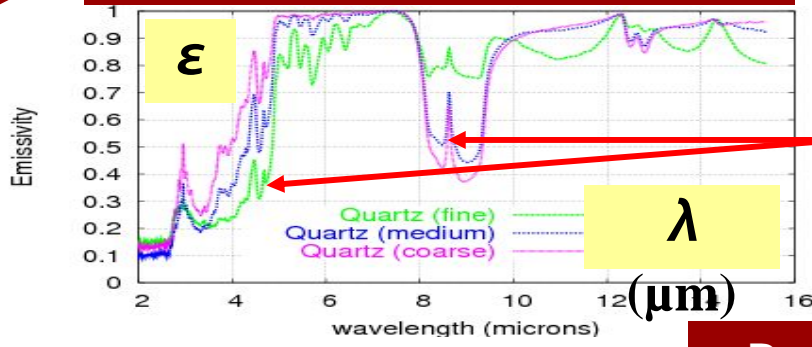
*<sup>a</sup> CNES - Centre Spatial de Toulouse, Toulouse, France*

*<sup>b</sup> Laboratoire de Météorologie Dynamique, IPSL, Ecole Polytechnique, Palaiseau, France.*

# Spectral variation of emissivity in TIR



## Bare soil: quartz

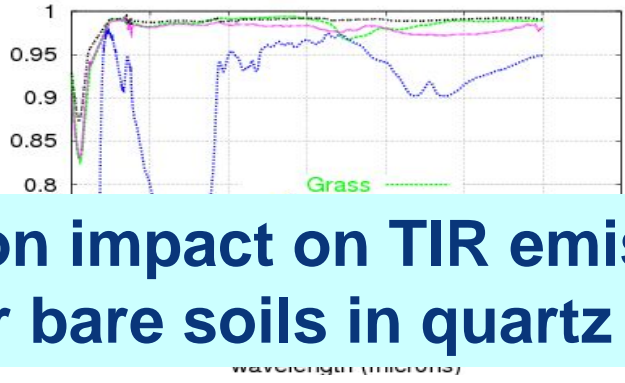
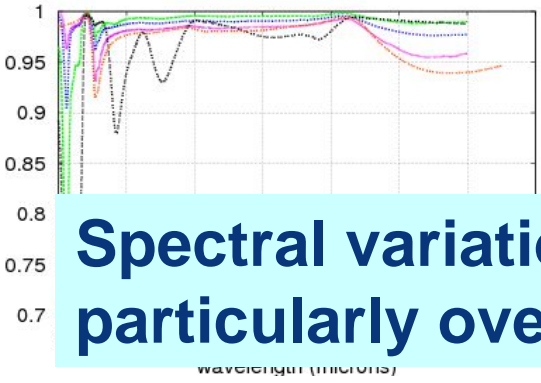


Quartz  
Reststrahlen  
bands

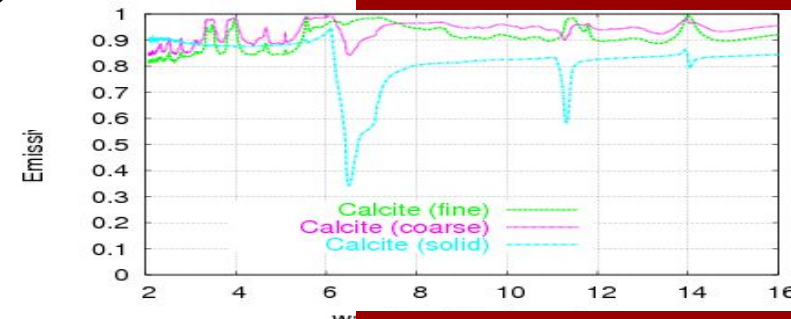
from MODIS/UCSB  
and ASTER/JPL  
emissivity libraries

## Snow and Ice

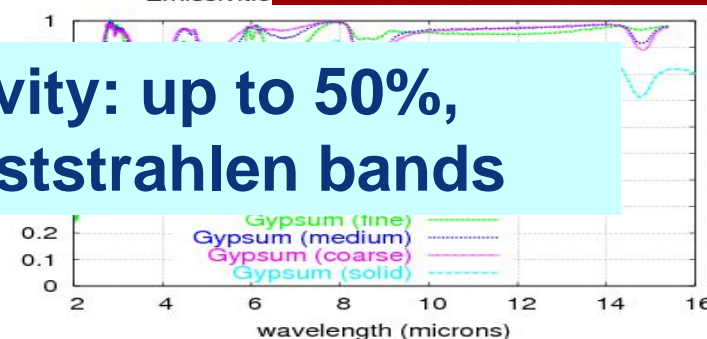
## Vegetation



## Bare soil: calcite

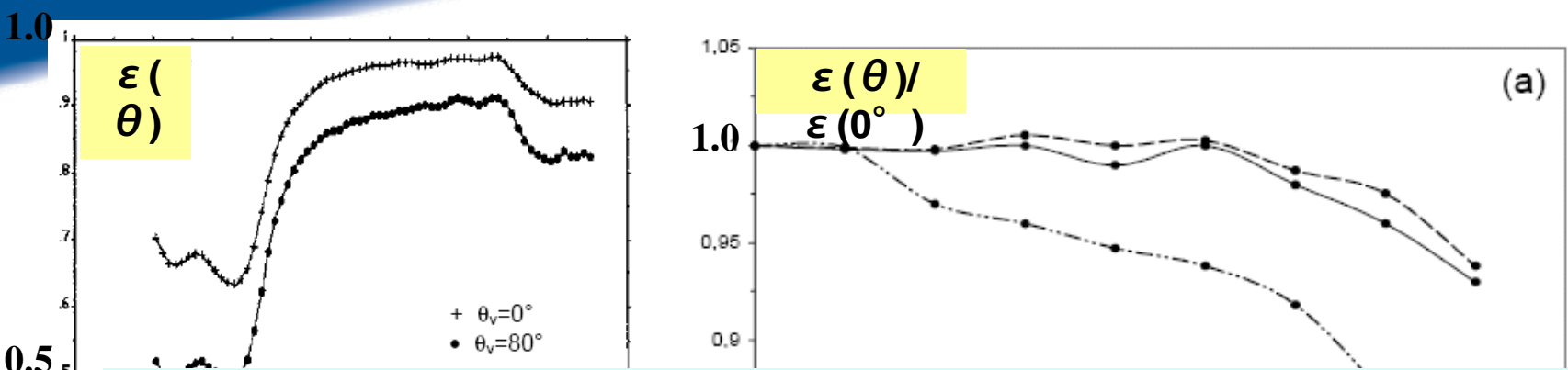


## Bare soil: gypsum



**Spectral variation impact on TIR emissivity: up to 50%, particularly over bare soils in quartz Reststrahlen bands**

# Angular variation of emissivity in TIR



**Angular variation impact on TIR emissivity: effect < 5% for  $\theta < 40^\circ$  .**

For IR sounders at 10km spatial resolution, this effect is even smaller (spatial averaging)

Conclusion : For IR sounders, emissivity angular variation is a 2<sup>nd</sup> order effect in comparison to spectral variation for viewing angles lower than  $40^\circ$  .

=> Lambertian assumption

# Infrared RTE (Lambertian surface, clear sky, night)

$$I(\lambda, \theta) = \varepsilon_s(\lambda) \tau_s(\lambda, \theta) B(\lambda, T_s)$$

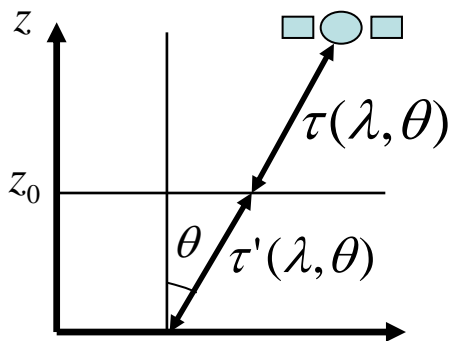
Surface Emission

$$+ \int_{\tau_s(\lambda, \theta)}^0 B[\lambda, T] \partial \tau(\lambda, \theta)$$

Upwelling Atmosphere Emission

$$+ (1 - \varepsilon_s(\lambda)) \tau_s(\lambda, \theta) \int_{\tau_s(\lambda, \theta)}^0 B[\lambda, T] \partial \tau'(\lambda, \theta)$$

Reflected Downwelling Atmosphere Emission for a Lambertian surface



$$\tau'(\lambda, \theta) \tau(\lambda, \theta) = \tau_s(\lambda, \theta)$$

## Multi Spectral Method (MSM)

*Péquignot et al. (2008), Infrared continental surface emissivity spectra retrieved from hyperspectral sensors. Application to AIRS. JAMC.*

$$\varepsilon_s(\lambda) = \frac{I(\lambda, \theta) - \int_{\tau_s(\lambda, \theta)}^0 B[\lambda, T] \partial \tau(\lambda, \theta) - \tau_s(\lambda, \theta) \int_{\tau_s(\lambda, \theta)}^0 B[\lambda, T] \partial \tau'(\lambda, \theta)}{\tau_s(\lambda, \theta) \left\{ B(\lambda, T_s) - \int_{\tau_s(\lambda, \theta)}^0 B[\lambda, T] \partial \tau'(\lambda, \theta) \right\}}$$

The formula holds only for **window channels**

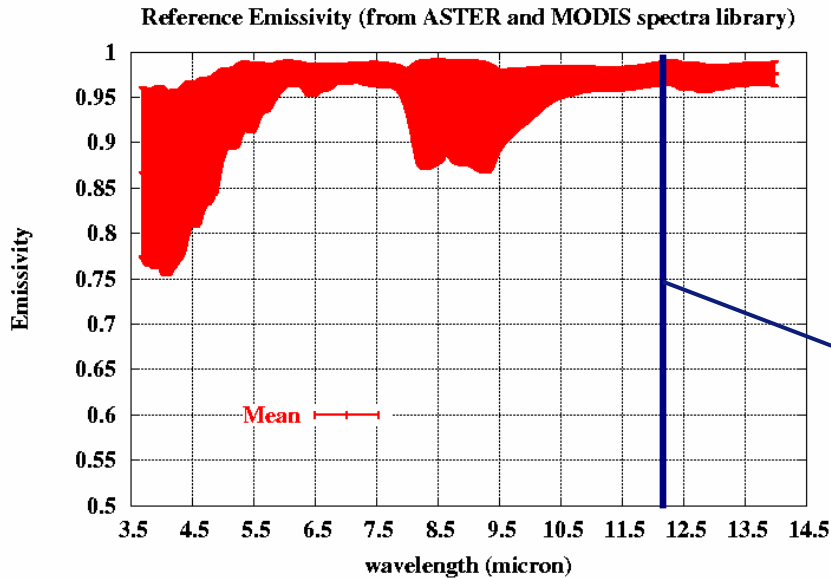
$$\tau_s(\lambda, \theta) \neq 0$$

In order to calculate  $\varepsilon_s$  one needs:

- 1) identifying clear sky radiances -> EUMETSAT IASI L2 cloud mask (based on AVHRR)
- 2) knowing the thermodynamic state of the atmosphere (T, H<sub>2</sub>O, O<sub>3</sub> profiles) -> EUMETSAT IASI L2 products
- 3) estimating the surface skin temperature

# Surface skin temperature :

## semi-transparent spectral band [ 12.12 - 12.22 $\mu\text{m}$ ]



Emmissivity variability ( $\mu \pm \sigma$ ) of the 8461 IASI channels calculated from soil and vegetation emissivity spectra of MODIS/UCSB and ASTER/JPL libraries

**Spectral band [12.12 - 12.22  $\mu\text{m}$ ],  
 $\lambda_0 = 12.17 \mu\text{m}$**

$\tau_s > 0.5$  and  $\epsilon \sim 0.97$

$$T_s = B^{-1} \left( \frac{I_{sat}(\lambda_0, \theta) - \int_{\tau_s(\lambda_0, \theta)}^1 B[\lambda_0, T(\tau(\lambda_0, \theta))] d\tau - (1 - \epsilon_s(\lambda_0)) \tau_s(\lambda_0, \theta) \int_{\tau_s(\lambda_0, \theta)}^1 B[\lambda_0, T(\tau'(\lambda_0, \theta))] d\tau'}{\epsilon_s(\lambda_0) \tau_s(\lambda_0, \theta)} \right)$$

right hand side calculated from EUMETSAT L2 atmospheric profiles using a Fast Radiative Transfer Model based on 4A “line-by-line” code (4A : [Scott and Chédin, 1981])

# Infrared Emissivity Spectrum from 3.7 to 14 $\mu\text{m}$

$$\varepsilon_s(\lambda) = \frac{I(\lambda, \theta) - \int_{\tau_s(\lambda, \theta)}^0 B[\lambda, T] \partial \tau(\lambda, \theta) - \tau_s(\lambda, \theta) \int_{\tau_s(\lambda, \theta)}^0 B[\lambda, T] \partial \tau'(\lambda, \theta)}{\tau_s(\lambda, \theta) \left\{ B(\lambda, T_s) - \int_{\tau_s(\lambda, \theta)}^0 B[\lambda, T] \partial \tau'(\lambda, \theta) \right\}}$$

$\varepsilon$  calculated for about 90 IASI channels selected for their high sensitivity to surface parameters

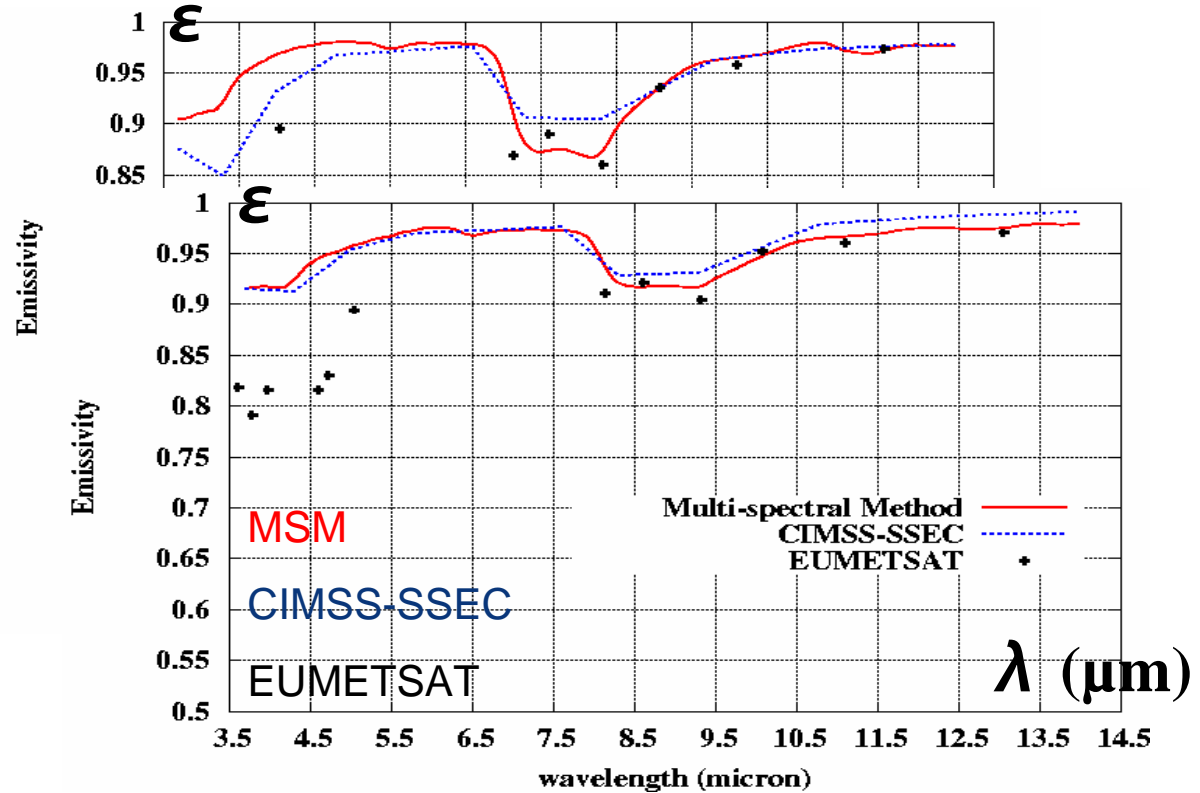
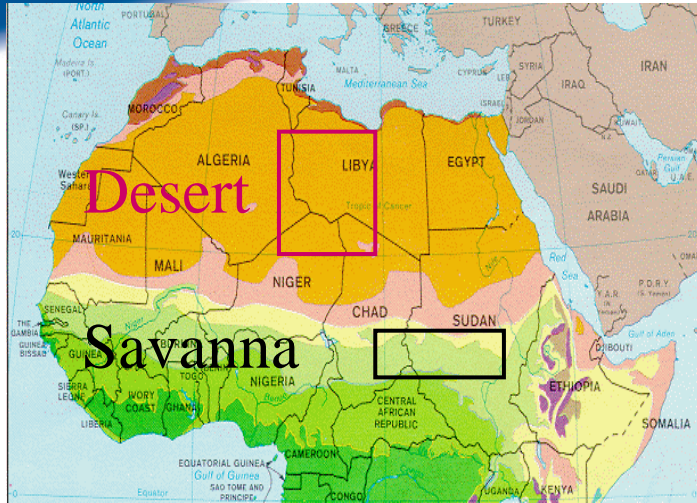
Least square minimization + shape adjustment

Emissivity continuous spectrum between 3.7 and 14.0  $\mu\text{m}$

## MSM Emissivity database :

- 165 spectra for various soil and vegetation types extracted from MODIS/UCSB and ASTER/JPL emissivity libraries.
- sampling : [3.70 - 14.0]  $\mu\text{m}$  at 0.05  $\mu\text{m}$  resolution.

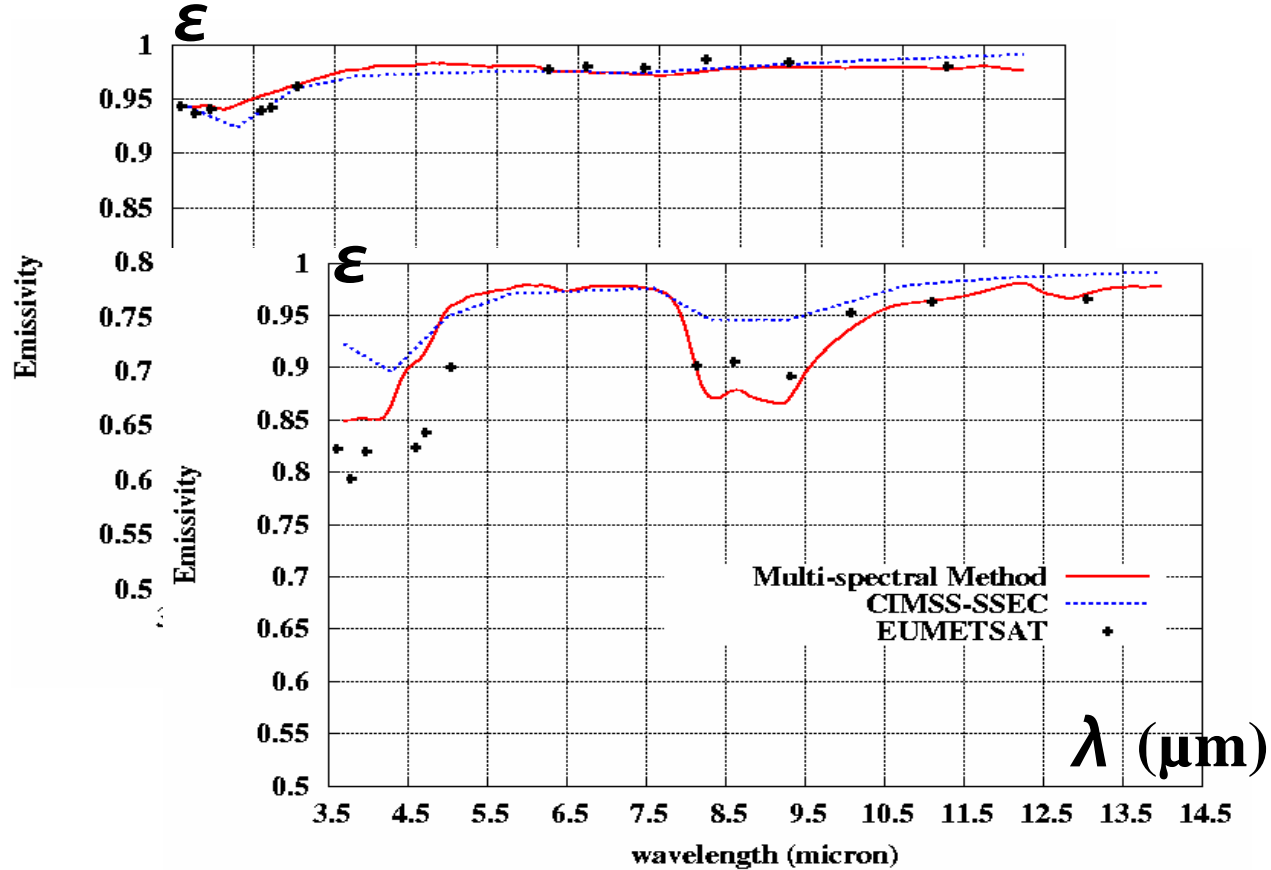
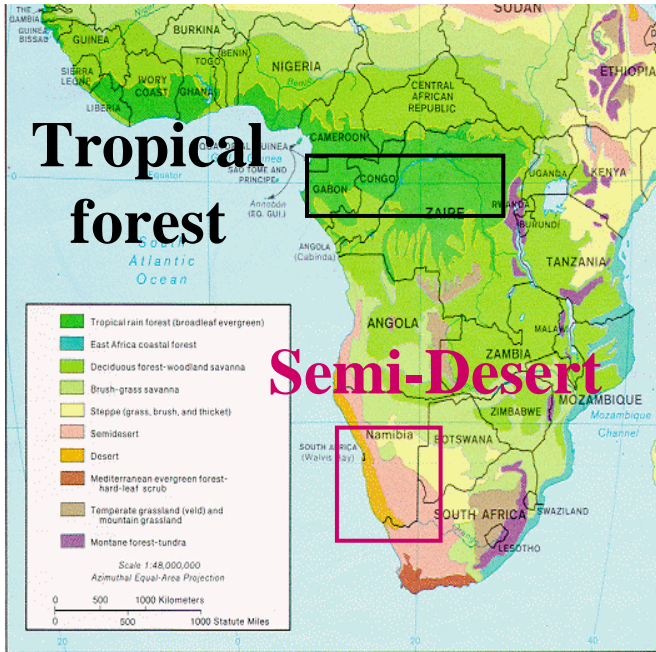
# Results for Jan 2008 (1<sup>st</sup>, 9<sup>th</sup>, 25<sup>th</sup>) : spectral variation (1)



- Quartz reststrahlen bands are well observed and dominate the  $\epsilon$  spectra
- In quartz reststrahlen bands  $\epsilon$  increases with the % of vegetation (Example of Savannas)



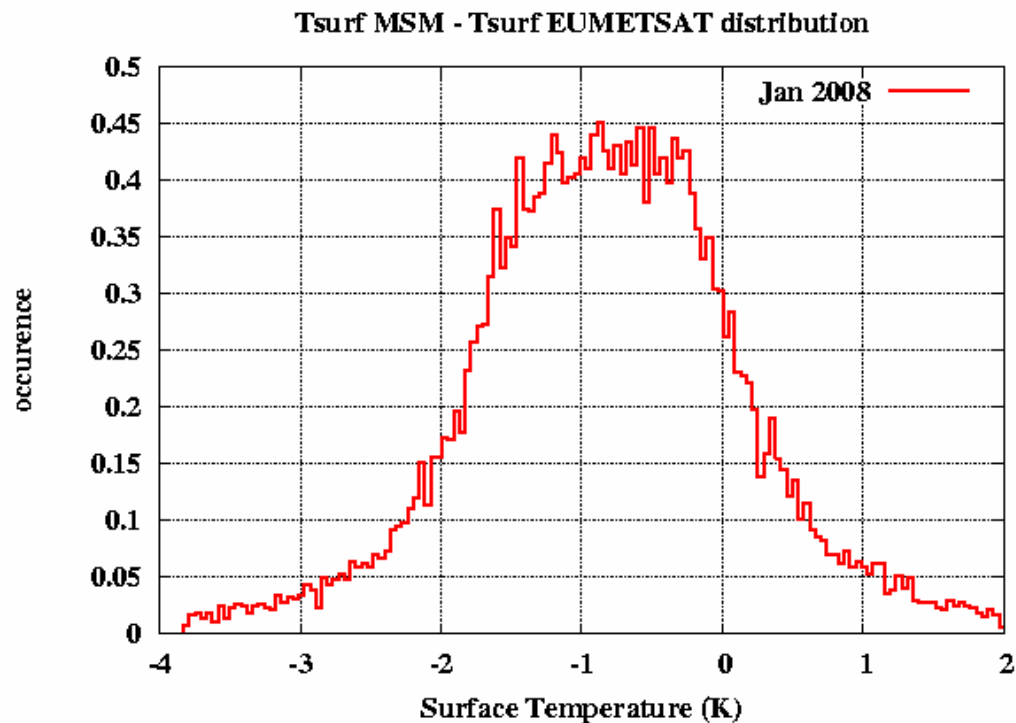
# Results for Jan 2008 (1<sup>st</sup>, 9<sup>th</sup>, 25<sup>th</sup>) : spectral variation (2)



- Tropical forest emissivity close to 1 (as expected)
- For semi-desert areas emissivity still influenced by quartz reststrahlen bands

## Results for Jan 2008 (1<sup>st</sup>, 9<sup>th</sup>, 25<sup>th</sup>) : surface temperature over land

Difference between  $T_{\text{surf}}$  calculated by MSM and  $T_{\text{surf}}$  provided by L2 - Eumetsat



$$\mu = -0.9 \text{ K}$$

$$\sigma = 1 \text{ K}$$

Values coherent with  
presently reported  
accuracies

# Expected accuracy on emissivity calculated by the MSM

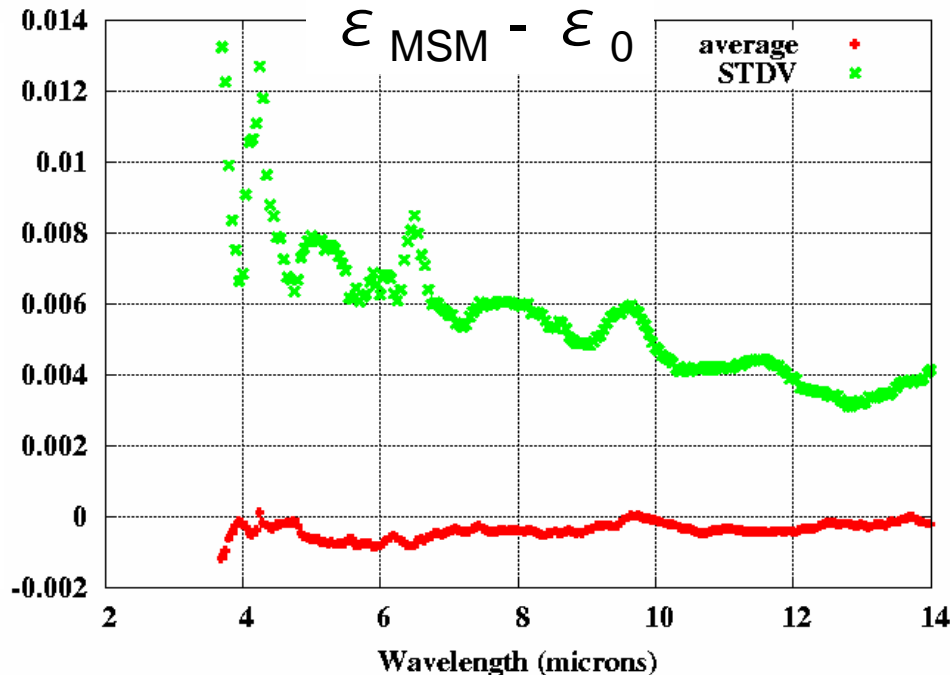
Statistics done on 10000 simulated cases :

For each simulation we have randomly chosen :

1/ an emissivity spectrum (MSM emissivity database)

2/ an atmospheric situation (TIGR dataset)

3/ a surface temperature defined as  $T_{\text{lowest\_level\_TIGR}} + \text{Gaussian}(\mu=0\text{K}, \sigma=4\text{K})$



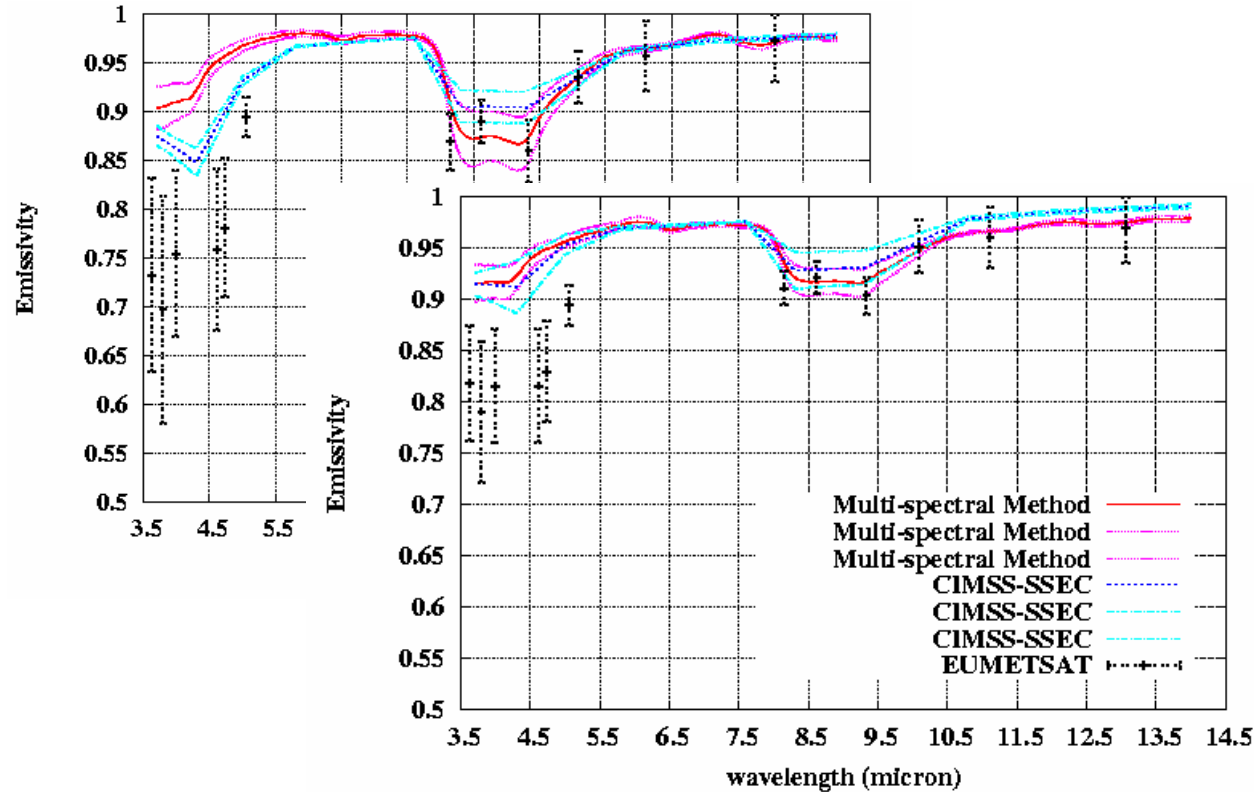
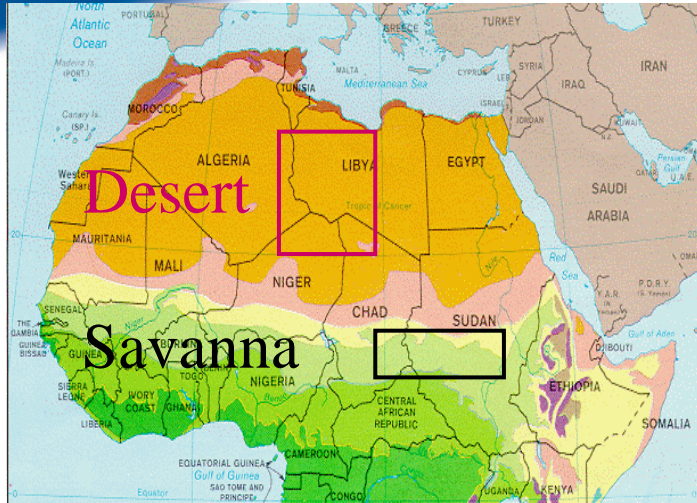
Theoretical accuracy on  $\epsilon$  : < 1.5%

Other effect has to be considered for operational processing :

- Residual clouds
- Potential wavelength dependant bias between radiative transfer simulations and observations
- Angular variation of  $\epsilon$

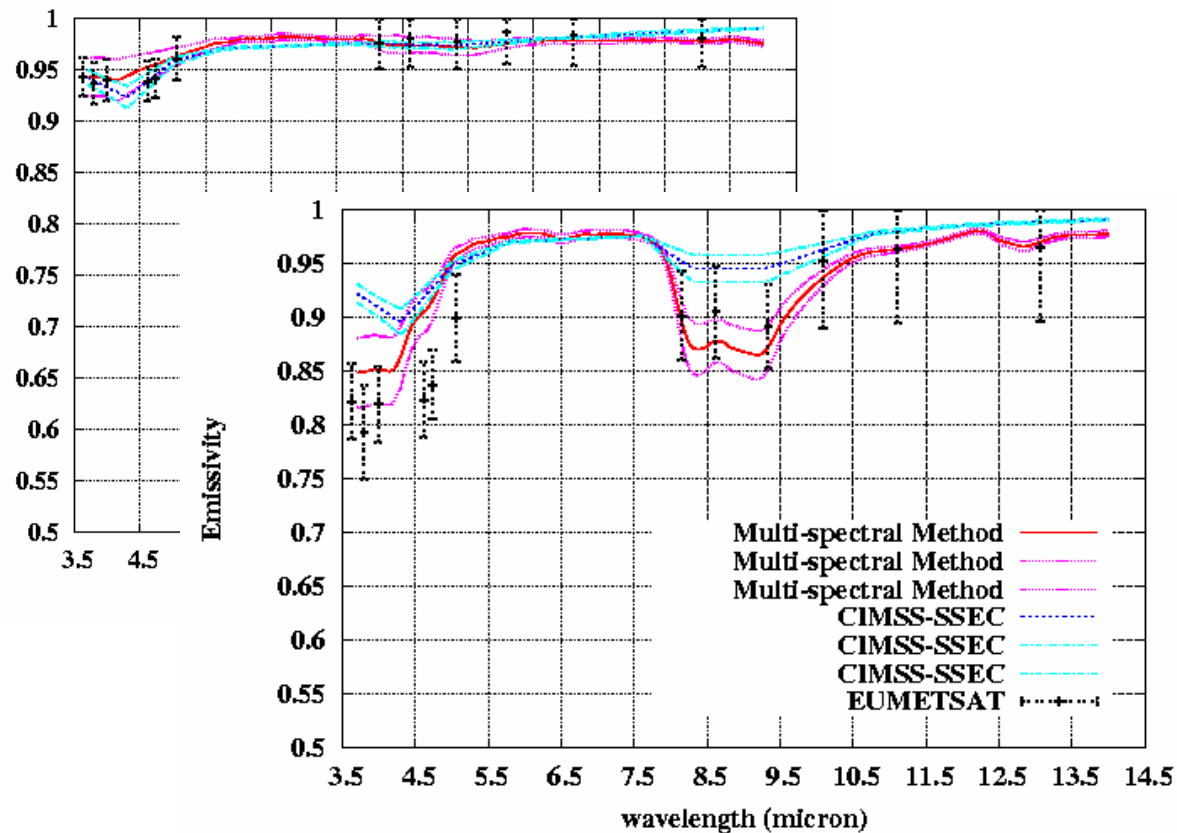
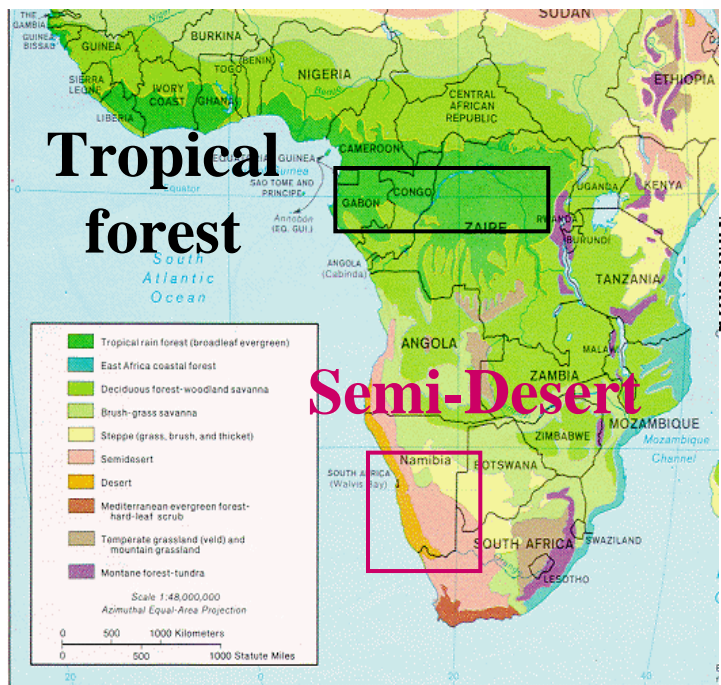
Expected effect (from AIRS experience) : error increase of about 25-50 % [Péquignot et al, 2008]

# Comparison with CIMSS and EUMETSAT L2



- Good agreement between MSM, CIMSS and EUMETSAT emissivities, except at 4  $\mu\text{m}$  (signal lower in that spectral region, emissivity harder to estimate)
- Lower spatial dispersion for CIMSS and MSM emissivity

# Comparison with CIMSS and EUMETSAT L2



## Conclusions

- 1) Emissivity Multi-Spectral Method (MSM) works well and is adapted to instruments with high spectral resolution.
- 2) We need to analyze more data to go further with comparisons and build a climatology of emissivity retrieved from IASI
- 3) Such emissivity spectra and surface skin temperature should help improving models of the earth surface-atmosphere interaction and the retrieval of meteorological profiles from infrared vertical sounders.
- 4) Easy to implement the Multi-Spectral Method in Near Real Time inversion data processing.